

# Pigment Epithelium–Derived Factor Is a Substrate for Matrix Metalloproteinase Type 2 and Type 9: Implications for Downregulation in Hypoxia

Luigi Notari,<sup>1</sup> Amanda Miller,<sup>1</sup> Alfredo Martínez,<sup>2,3</sup> Juan Amaral,<sup>1</sup> Meibua Ju,<sup>4</sup> Gregory Robinson,<sup>4</sup> Lois E. H. Smith,<sup>4</sup> and S. Patricia Becerra<sup>1</sup>

**PURPOSE.** Pigment epithelium–derived factor (PEDF), a protein secreted by the retinal pigment epithelium (RPE), acts on retinal survival and angiogenesis. Because hypoxia and VEGF regulate matrix metalloproteinases (MMPs), their effects on PEDF proteolysis were explored.

**METHODS.** Mouse models for retinopathy of prematurity (ROP) were used. Cultured monkey RPE cells were exposed to low oxygen and chemical hypoxia mimetics. *PEDF* and *VEGF* mRNA levels in RPE were determined by RT-PCR. MMPs were assessed by zymography, DQ-gelatin degradation solution assays, and MMP immunostaining. PEDF proteolysis was assayed in solution and followed by SDS-PAGE and immunostaining. MMP induction by VEGF was performed in baby hamster kidney (BHK) cells. Retinal R28 cell survival, ex vivo chick embryonic aortic vessel sprouting, and directed in vivo angiogenesis assays were performed.

**RESULTS.** Levels of PEDF in RPE/choroid significantly decreased in the ROP model. Hypoxia decreased PEDF levels in the media conditioned by RPE cells, with no significant change in *PEDF* mRNA. Conversely, PEDF proteolysis, gelatinolytic activities of ~57-kDa and ~86-kDa zymogens, and MMP-2 immunoreactivities increased with hypoxia. Addition of VEGF to BHK cells caused a time and dose-related upregulation of ~57-kDa zymogens and of DQ-gelatinolytic and PEDF-degrading activity. The PEDF-degrading activity and ~57-kDa zymogens in the BHK media shared MMP protease inhibition patterns and MMP-2 immunoreactivities with those in the vitreous. Limited proteolysis with MMP-2 and -9 degraded PEDF in a Ca<sup>2+</sup>-dependent fashion. MMP-mediated proteolysis of PEDF abolished the retinal survival and antiangiogenic activities of the PEDF protein.

**CONCLUSIONS.** Hypoxia and VEGF can downregulate PEDF through proteolytic degradation. PEDF is a novel substrate for MMP-2 and -9. These results reveal a novel posttranslational mechanism for downregulating PEDF, and provide an explanation for hypoxia-provoked increases in VEGF/PEDF ratios, in

angiogenesis and/or in neuronal death. (*Invest Ophthalmol Vis Sci.* 2005;46:2736–2747) DOI:10.1167/iovs.041489

Pigment epithelium-derived factor (PEDF) is the principal antiangiogenic and neurotrophic protein of the eye.<sup>1–3</sup> It is highly expressed in the retinal pigment epithelium (RPE)<sup>4–6</sup> and the secreted product associates with components of the extracellular matrix (ECM) in the proximal interphotoreceptor matrix and vitreous.<sup>7–9</sup> Extracellular PEDF acts to promote neuronal survival and differentiation in the retina and central nervous system (CNS),<sup>2</sup> and it excludes vessels from invading the retina, vitreous, and cornea.<sup>1</sup> Overexpression of PEDF efficiently protects against cell death from retinal ischemia and photoreceptor degeneration, inhibits choroidal and retinal neovascularization, and suppresses tumor angiogenesis and growth.<sup>10–14</sup> Conversely, suppression of PEDF in the retina correlates with formation of choroidal neovascularization, and PEDF correlates positively with oxygen concentrations, suggesting that PEDF loss plays a permissive role in ischemia-driven retinal neovascularization.<sup>15–18</sup>

PEDF is a 50-kDa glycoprotein and a noninhibitory member of the serpin superfamily of proteins related through their highly conserved folded protein conformation.<sup>19,20</sup> Comparison of the PEDF structure with known structures of other native serpins (e.g., the  $\alpha_1$ -proteinase inhibitor, ovalbumin) has shown a high level of structural conservation, despite the relatively low sequence identity among these family members (20%–27% for these serpins).<sup>21</sup> However, unlike most serpins, PEDF acts as a substrate rather than an inhibitor of serine proteases.<sup>22</sup> The compact and globular PEDF protein is highly resistant to proteolytic cleavage, with the exception of a protease-sensitive exposed peptide loop located toward its C-end. On cleavage by serine proteases, subtilisin, or endoproteases, the limited PEDF polypeptide products (~46-kDa) retain biological activity and binding affinity for ECM collagens and glycosaminoglycans.<sup>8,9,22</sup>

There is increasing evidence of the involvement of ECM degradation in stimulation of angiogenesis and cell injury. Expression of matrix metalloproteinases type 2 (MMP-2) and type 9 (MMP-9) correlates with the progression of neovascular diseases.<sup>23–25</sup> These metalloproteinases are upregulated not only in angiogenic lesions but also in retinal ganglion cell (RGC) death, and their inhibition or genetic ablation diminishes angiogenic switching, tumor number, and growth<sup>26,27</sup> and also protects against pathologic RGC death.<sup>28</sup> MMP-2 and -9 belong to the MMP family of highly conserved Zn<sup>2+</sup>- and Ca<sup>2+</sup>-dependent extracellular peptidases.<sup>29</sup> They degrade most ECM components and many non-ECM molecules, thereby allowing cell migration and modulation of biologically active molecules by direct cleavage or by release from ECM stores.<sup>30,31</sup> A group of these bioactive molecules are proangiogenic factors (e.g., the VEGF and FGF families), which under hypoxic conditions are upregulated and in turn can stimulate proliferation and proteolysis-associated migration of endothelial cells.<sup>32–36</sup> At the same time, VEGF and FGFs can induce expression of MMPs.

From the <sup>1</sup>Laboratory of Retinal Cell and Molecular Biology, National Eye Institute, and the <sup>2</sup>Cell and Cancer Biology Branch, National Cancer Institute, National Institutes of Health, Bethesda, Maryland; and the <sup>4</sup>Department of Ophthalmology, Children's Hospital, Harvard Medical School, Boston, Massachusetts.

<sup>3</sup>Present affiliation: Department of Neuroanatomy and Cell Biology, Instituto Cajal, CSIC, Madrid, Spain.

Submitted for publication December 17, 2004; revised March 10, 2005; accepted April 26, 2005.

Disclosure: L. Notari, None; A. Miller, None; A. Martínez, None; J. Amaral, None; M. Ju, None; G. Robinson, None; L.E.H. Smith, None; S.P. Becerra, None

The publication costs of this article were defrayed in part by page charge payment. This article must therefore be marked "advertisement" in accordance with 18 U.S.C. §1734 solely to indicate this fact.

Corresponding author: S. Patricia Becerra, Laboratory of Retinal Cell and Molecular Biology, National Eye Institute, National Institutes of Health, Building 7, Room 304, 7 Memorial Drive MSC 0607, Bethesda, MD, 20892-0607; becerrap@nei.nih.gov.

However, angiogenic control depends not only on increases and availability of positive factors for angiogenesis but on the correct balance between anti- and proangiogenic factors, as neovascularization-related diseases correlate with loss of this balance.<sup>37-39</sup>

Given that PEDF and MMPs coexist in the ECM and both participate in modulation of angiogenesis and cell injury, it was of interest to investigate the effects of extracellular matrix metalloproteinases on PEDF. We showed that PEDF is a substrate for MMP-2 and -9 and that induction of MMPs by hypoxia or exogenous addition of VEGF provokes degradation of PEDF protein in extracellular compartments. The data provide a model for molecular players that control the hypoxia-provoked increases in the VEGF-PEDF ratio, angiogenesis, and/or neuronal death and suggest that PEDF degradation by MMP is a novel component of the angiogenic switch and can control retinal survival.

## METHODS

### PEDF Protein

Recombinant human (rhu)PEDF protein was purified from the culture medium of baby hamster kidney (BHK) cells containing an expression vector for human PEDF, as described.<sup>40</sup> To remove any residual MMPs from the rhuPEDF sample, gelatin affinity column chromatography using gelatin-Sepharose (Sigma-Aldrich, St. Louis, MO) was performed according to a method described previously,<sup>41</sup> with minor modifications. Briefly, 1 mg of rhuPEDF (1 mL volume) was applied to a gelatin Sepharose column (2 mL-column bed; Amersham Bioscience, Piscataway, NJ) pre-equilibrated with buffer A (0.05 M Tris-HCl [pH 7.5] and 1 M NaCl). The column was washed with five column volumes of buffer A and then with 1.5 M NaCl in buffer A, followed by elution of MMP proteins with 5% dimethyl sulfoxide (DMSO) in 1.5 M NaCl and buffer A. Fractions corresponding to flow-through and initial wash of the column were collected and reloaded, and the washes and elutions repeated. The flow-through and washes containing PEDF free of MMPs were collected and concentrated by ultrafiltration (Centricon-30; Amicon, Beverly, MA). The final concentrated sample contained 0.7 mg of purified rhuPEDF.

### Oxygen-Induced Retinopathy in the Mouse

The retinopathy of prematurity (ROP) mouse model was developed by a method performed as described before<sup>42</sup> and in which retinal ischemia, neovascularization and neuronal cell death are induced on removing the animals from 75% oxygen to normoxia. Briefly, C57BL/6 mice with nursing mother were exposed to 75% oxygen from postnatal day (P)7 to P12. At P8 (hyperoxia), P13, P17, and P21 (retinal ischemia) and their corresponding normoxia control group, four animals from different litters were anesthetized with tribromoethanol (Avertin; Sigma-Aldrich), and the eyes were enucleated. Retina and RPE/choroid layers were separated by dissection, pooled, and processed immediately. For each layer, one fifth of the tissue was transferred immediately into lysis buffer (RLT; Qiagen, Valencia, CA) to extract RNA. The remaining tissue was transferred into protein lysis buffer containing 62.5 mM Tris (pH 7.0), 2% SDS, 10% glycerol and 1× protease inhibitor (Complete; Sigma-Aldrich); and, after protein determination, 100 mM DTT and 0.01% bromophenol blue dye were added to each extract in preparation for SDS-PAGE. This protocol was performed in compliance with the ARVO Statement for the Use of Animals in Ophthalmic and Vision Research.

### Hypoxic Treatment of Monkey RPE Cells

Monkey RPE cells were nontransformed at an early passage and were the generous gift of Bruce Pfeiffer (Bausch & Lomb, Rochester, NY).<sup>4</sup> RPE cells were cultured in D-MEM/F12 in a 1:1 mixture, supplemented with 5% fetal bovine serum (FBS), 1.5 mM L-glutamine, 7.5 mM sodium

pyruvate, 0.1 mM nonessential amino acids, and penicillin-streptomycin (100 U/mL and 100 mg/mL, respectively). Cells were incubated at 37°C in the presence of 5% CO<sub>2</sub>.

To study the effect of oxygen on PEDF production, RPE cells were incubated in a sealed chamber at 37°C for 48 hours in a controlled environment of 1% or 7% O<sub>2</sub> in the presence of 5% CO<sub>2</sub> and 94% or 88% N<sub>2</sub>, respectively, as described.<sup>43</sup> Cells cultured under standard conditions (21% O<sub>2</sub>, 5% CO<sub>2</sub>, and 74% N<sub>2</sub>) served as normoxia control cultures. Hypoxic conditions were also mimicked by adding 100 μM CoCl<sub>2</sub>, an iron analogue, or 260 μM deferoxamine mesylate (DFM), an iron chelator, to the culture media and incubating the cells at 37°C for 48 hours, as described.<sup>43</sup> After treatment, the cells and medium were separated by centrifugation. The medium was concentrated 80-fold by ultrafiltration using concentrators (Centricon-30; Amicon) and contained less than 5 μg/mL PEDF. The cells were washed with phosphate-buffered saline (PBS), harvested, and stored frozen at -70°C.

### Quantitative Real-Time PCR

mRNA expression levels were determined by quantitative real-time PCR. PCR primers and probes targeting experimental and control genes, 18S ribosomal RNA, and cyclophilin were designed on computer (Primer Express software; Applied Biosystems, Inc. [ABI], Foster City, CA). Primers were synthesized by Oligo Therapeutics (La Jolla, CA) and had the following murine sequences: PEDF forward primer, 5'-AGGACATGAAGCTACAGTCGGTTGTT-3' and reverse primer, 5'-CTC-GAAAGCAGCCCTGTGTT-3'; VEGF forward primer, 5'-GGAGATC-CTTCGAGGAGCACTT-3', and reverse primer, 5'-GGCGATTTAGC-AGCAGATATAAGAA-3'; and cyclophilin A (reference gene or normalizer) forward primer, 5'-CAGACGCCACTGTGCTTTT-3', and reverse primer, 5'-TGTCCTTTGGAACCTTGTCTGCAA-3'. Primer and probe sequences were analyzed for specificity of gene detection by means of the BLAST module (National Center for Biotechnology Information, Bethesda, MD) and the first derivative primer melting-curve software supplied by ABI. This analysis determines the presence of amplicons based on their specific melting-point temperatures. In addition, all PCR amplicons were sequenced and matched with the published gene sequence. Analysis of gene expression was generated on a sequence-detection system (Prism 7700, with *TaqMan*; ABI). A standard curve representing four 4-fold dilutions of stock cDNA (1:2.5, 1:10, 1:40, and 1:160) was used for linear regression analysis of unknown samples. All changes in gene expression are normalized to cyclophilin or 18S and expressed as relative units, unless otherwise described. Each qRT-PCR analysis was repeated to ensure reproducibility.

### PEDF Proteolytic Degradation Solution Assays

Purified rhuPEDF was mixed with purified recombinant human MMP-2 (catalog no. PF023; Oncogene Research Products, Boston, MA) or recombinant human MMP-9 (catalog no. PF024; Oncogene) in PBS at a variety of substrate-to-proteinase ratios (wt/wt). Similarly, degradation of PEDF was assayed in PEDF-containing conditioned medium or vitreous in the absence or presence of AEBSF (4-(2-aminoethyl)benzenesulphonyl fluoride; MP Biomedical, Irvine, CA), aprotinin (Sigma-Aldrich), pepstatin A (Roche Molecular Biochemicals, Indianapolis, IN), leupeptin (MP Biomedical), E-64 (Roche Molecular Biochemicals), and EDTA (Sigma-Aldrich). After incubation at 37°C for indicated lengths of time (see legend to Figs. 4C, 4D, and 4E), the reactions were stopped by adding SDS-sample buffer and freezing. Proteins in the mixtures were subjected to SDS-PAGE using 10% to 20% polyacrylamide gradient gels (Invitrogen, Carlsbad, CA) and then either stained with Coomassie blue or transferred to nitrocellulose membranes for immunostaining with antibody to PEDF.

### BHK[pPEDF] Cell Culture

BHK[pMA-PEDF] cells<sup>40</sup> were cultured in DMEM supplemented with 10% FBS, penicillin-streptomycin (100 U/mL and 100 mg/mL, respectively), 0.4 mg/mL G418, and 4.5 mg/mL methotrexate. Cells were

incubated in 12-well plates at 37°C in the presence of 5% CO<sub>2</sub>. After 24 hours of incubation without serum, the culture media contained less than 0.4 µg/mL PEDF protein.

For MMP induction, BHK[pMA-PEDF] cells were cultured to confluence and the media replaced with serum-free media containing indicated concentrations of recombinant human VEGF (R&D Systems, Minneapolis, MN). The conditioned media were collected after incubation for 1, 2, 4, 8, and 24 hours at 37°C in the presence of 5% CO<sub>2</sub>. At each time point, the number of cells remained constant among all treatments, even with the highest concentrations of VEGF.

### Preparation of Vitreous Extracts

Monkey eyes were obtained from the Diagnostic and Research Services Branch, Veterinary Resources Program, National Institutes of Health. Vitreous extracts from monkey eyes were prepared as described before.<sup>44</sup> Briefly, after dissection of the anterior segment of the eye, the vitreous gel was transferred to a tube, homogenized (Polytron, Brinkman Instruments, Westbury, NY), and subjected to centrifugation at 1300g for 15 minutes at 4°C. The supernatant contained ~0.4 mg/mL protein and was fractionated by 45% to 70% ammonium sulfate precipitation. The precipitated fraction (termed p70) was dissolved, dialyzed against PBS, and concentrated by ultrafiltration with centrifugal filter devices (Amicon Ultra-4; 10K NMWL; Millipore, Bedford, MA) to a final concentration of 1 to 6 mg/mL protein. Fraction p70 contained PEDF and MMP-2 proteinases as previously described.<sup>44,45</sup>

### Gelatin Zymography

The activity of proteases was detected by gelatin zymography,<sup>44</sup> performed on premade 10% polyacrylamide gels containing 0.1% gelatin with Tris-glycine running buffer (Invitrogen). After electrophoresis, gels were incubated in renaturing buffer at room temperature for 1 hour and then incubated in developing buffer containing 5 mM CaCl<sub>2</sub> at 37°C for 16 hours. For assaying zymogen inhibition, a specific proteases inhibitor—EDTA (20 mM), calpain inhibitor E-64 (10 µg/mL), AEBSF (100 mM), aprotinin (5 µg/mL), pepstatin A (5 µg/mL), or leupeptin (5 µg/mL)—was added to the developing buffer. To visualize the zymogen bands, gels were stained with 0.5% Coomassie blue R-250 in 50% methanol/10% acetic acid for 30 minutes and then destained in 10% methanol/10% isopropanol for 2 hours at room temperature with gentle shaking.

### DQ-Gelatin Degradation Solution Assays

The conditioned media of BHK[pPEDF] cells (10 µL) were incubated with 20 µL of DQ-gelatin substrate (Molecular Probes, Inc., Eugene, OR) in reaction buffer containing 50 mM Tris-HCl (pH 7.6), 150 mM NaCl, 5 mM CaCl<sub>2</sub> (200 µL final volume), in accordance with the manufacturer's protocol. Increase in fluorescence at 515 nm due to the DQ-gelatin degradation by the overall gelatinase activities present in the conditioned medium was monitored in triplicate in 96-well plates (Victor<sup>2</sup> 1420 Multilabel Counter; Perkin Elmer Life Sciences, Boston, MA).

### Western Blot Analysis

Proteins were resolved by polyacrylamide gel electrophoresis with premade 10% to 20% polyacrylamide gels (Invitrogen) with tricine-SDS running buffer, according to the manufacturer's instructions. Proteins in gels were transferred to nitrocellulose membranes (pore size of 0.2 µm; Protran; Schleicher & Schuell, Keene, NH), and immunoreactions with anti-PEDF or anti-MMPs were performed as follows. The membranes were incubated in a 1:1000 dilution of mouse monoclonal anti-PEDF (Chemicon, Temecula, CA); 1: 4000 dilution of rabbit polyclonal antiserum against an rhuPEDF protein, Ab-rPEDF<sup>46</sup>; 1:1000 dilution of goat anti-human MMP-2 (Santa Cruz Biotechnology, Santa Cruz, CA); or 1:1000 dilution of goat anti-human MMP-9 (Santa Cruz Biotechnology) in 5% BSA in TBS-Tween (50 mM Tris-HCl [pH 7.5], 150 mM NaCl, and 0.1% Tween-20; Calbiochem, La Jolla, CA). After washes

with TBS-Tween, membranes were incubated in secondary antibody, rabbit anti-mouse biotinylated IgG-POD diluted at 1:1,000 (Vector Laboratories, Burlingame, CA) or rabbit anti-goat IgG horseradish peroxidase (HRP) diluted 1:100,000 (Santa Cruz Biotechnology). Immunoreactive bands were detected by chemiluminescence (Lumi-Light Plus; Roche Diagnostics). Alternatively, immunoreacted proteins were visualized by a colorimetric method by incubation with a biotinylated secondary antibody followed by incubation with streptavidin-HRP complex (ABC Elite Kit, Vectastain; Vector Laboratories) and color development with 4-chloro-naphthol (HRP color development reagent; Bio-Rad, Hercules, CA). Both monoclonal anti-PEDF and polyclonal Ab-rPEDF antibodies showed similar specificity and sensitivity of detection of PEDF protein from human and monkey sources used in the study.

### Quantification of Bands

Quantification of bands from Western blot or gelatin zymography was performed by digitizing the signals with a scanner (ScanJet; Hewlett Packard, Palo Alto, CA) and saving them as TIFF files at different exposure conditions (Photoshop; Adobe Systems, Inc., Mountain View, CA). For the zymographic analysis, negative images of the zymogens were obtained. The mean density of pixels and area of each band was determined with NIH Image software (available by ftp at [zippy.nimh.nih.gov/](http://zippy.nimh.nih.gov/) or at <http://rsb.info.nih.gov/nih-image/>; developed by Wayne Rasband, National Institutes of Health, Bethesda, MD). Background subtraction was performed before quantification of pixel density determination, when needed. The averages of more than two measurements per band and standard errors were calculated and plots were obtained by computer (Excel; Microsoft, Redmond, WA).

### Retinal Cell Survival Activity Assay

R28 cells, an immortalized retinal precursor cell line, were the kind gift of Gail M. Seigel (SUNY, Buffalo, NY). R28 cells were cultured in DMEM/F12 medium in a 1:1 mixture, supplemented with 5% FBS, 1.5 mM L-glutamine, 7.5 mM sodium pyruvate, 0.1 mM nonessential amino acids, 100 U/mL penicillin, and 100 mg/mL streptomycin. Cells were incubated at 37°C in the presence of 5% CO<sub>2</sub>. To induce cell death, R28 cells at subconfluence were deprived of serum as described by Barber et al.,<sup>47</sup> with minor modifications. Briefly, when R28 cell cultures reached 70% confluence in 24-well plates, serum-containing medium was removed, adherent cells were washed with PBS (pH 7.4) twice, and 400 µL of serum-free medium or 400 µL of serum-free medium containing PEDF test samples was added to each well. After incubation for 72 hours, cells were monitored using an inverted microscope (Olympus, Lake Success, NY) and representative fields were photographed. At the same time, cell viability was quantified by using a homogeneous method of determining the number of viable cells in culture based on quantitation of the adenosine triphosphate (ATP) present, an indicator of metabolically active cells. A cell viability kit (Cell Titer Glo; Promega, Madison, WI) was used according to the manufacturer's instructions. Luminescence due to the luciferin/luciferase reaction with the ATP present in the viable cells was measured with the plate reader (Victor<sup>2</sup> Multilabel; Perkin Elmer Life Sciences). Experiments were repeated four times each, with more than three replicates per point. Data were normalized to control data without effectors, average, standard deviations, and statistical parameters were calculated, and the changes over the control (*x*-fold) without effectors were plotted on computer (Excel; Microsoft).

### Chick Embryo Aortic Arch Assay

The chick embryo aortic arch assay is an *ex vivo* angiogenesis assay that was performed as previously described.<sup>48</sup> Briefly, aortic rings of approximately 0.8 mm in length were prepared from the five aortic arches of 13-day-old chicken embryos (CBT Farms, Chestertown, MD), and the soft connective tissue of the adventitia layer was carefully removed with tweezers. Each aortic ring was placed in the center of a well in a 48-well plate and covered with 10 µL of synthetic matrix

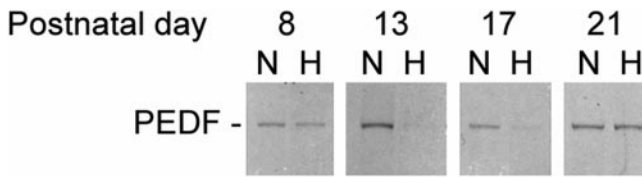


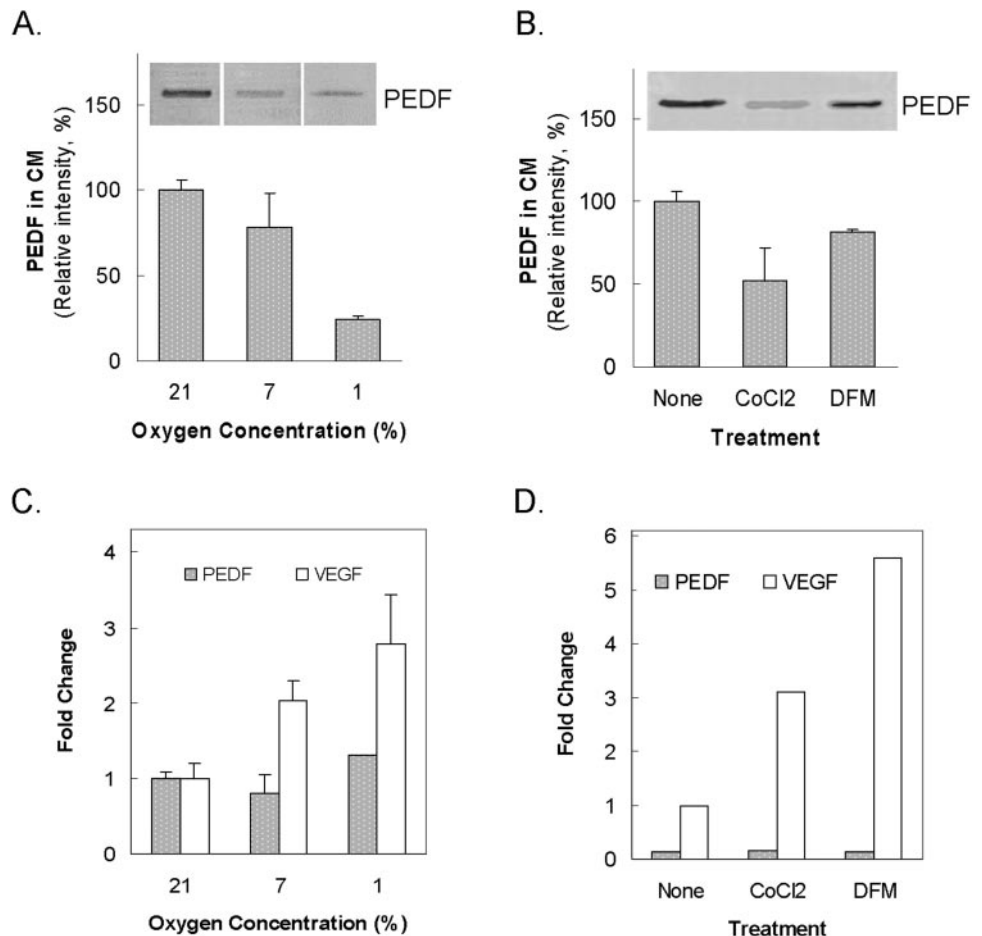
**FIGURE 1.** PEDF levels in the RPE-choroid of a mouse model of ROP. One-week-old C57BL/6J mice were exposed to 75% oxygen for 5 days between P7 and P12 and then to room air, to induce ischemia in the retina. At each different time point, RPE-choroid tissues from four eyes were microdissected and pooled, and proteins were extracted. Equivalent amounts of total protein (15  $\mu$ g) were loaded in polyacrylamide gels. Western blot analysis of RPE-choroid extracts from normoxic (N) and ischemic (H) animals, with a polyclonal antiserum to rhuPEDF, Ab-rPEDF, are shown.

(Matrigel; BD Biosciences, San Jose, CA). After the matrix solidified, 300  $\mu$ L of growth-factor-free human endothelial serum-free basal growth medium (Invitrogen) containing the proper concentration of the test substances was added to each well. The plates were kept in a humid incubator at 37°C in 5% CO<sub>2</sub> for 24 to 36 hours. Microvessels sprouting from each aortic ring were photographed in an inverted microscope and the area covered by the newly formed capillaries was estimated as reported.<sup>48</sup> Endothelial cell growth supplement (ECGS; Biomedical Collaborative Products, Bedford, MA) was used at 400  $\mu$ g/mL as an angiogenesis promoter. Six independent rings per treatment were measured.

### Directed In Vivo Angiogenesis Assay

Analysis and quantitation of angiogenesis was done using a directed in vivo angiogenesis assay (DIVAA) as previously described.<sup>49</sup>

**FIGURE 2.** Effect of hypoxia on PEDF in monkey retinal pigment epithelial (RPE) cells. The effects of decreasing oxygen concentrations (A, C) or chemically mimicking hypoxic conditions (B, D) on *PEDF* gene expression and on PEDF protein production are shown. RPE cells were exposed to various concentrations of oxygen or to the chemical reagents CoCl<sub>2</sub> and DFM, to mimic hypoxic conditions. Each treatment was performed in triplicate with the same batch of cells. (A, B) The culture medium from treated and untreated cells was concentrated (80-fold) and subjected to Western blot analysis and immunostaining with Ab-rPEDF by a colorimetric method. To quantify the amount of PEDF protein produced by RPE, the intensities of individual PEDF-immunoreactive bands were measured in three or four independent experiments with different batches of cells. The percentages of average intensities for PEDF protein for each treatment over the one in normoxia (labeled as 21) were plotted. (C, D) Quantitative RT-PCR was performed to measure the amount of *PEDF* and *VEGF* mRNA in treated and untreated cell pellets. The amount of RNA, expressed in relative units (normalized to cyclophilin) for each treatment, is shown. The intrameasurement error in all samples was <3%. VEGF, a hypoxia-induced gene, was monitored as the positive control.

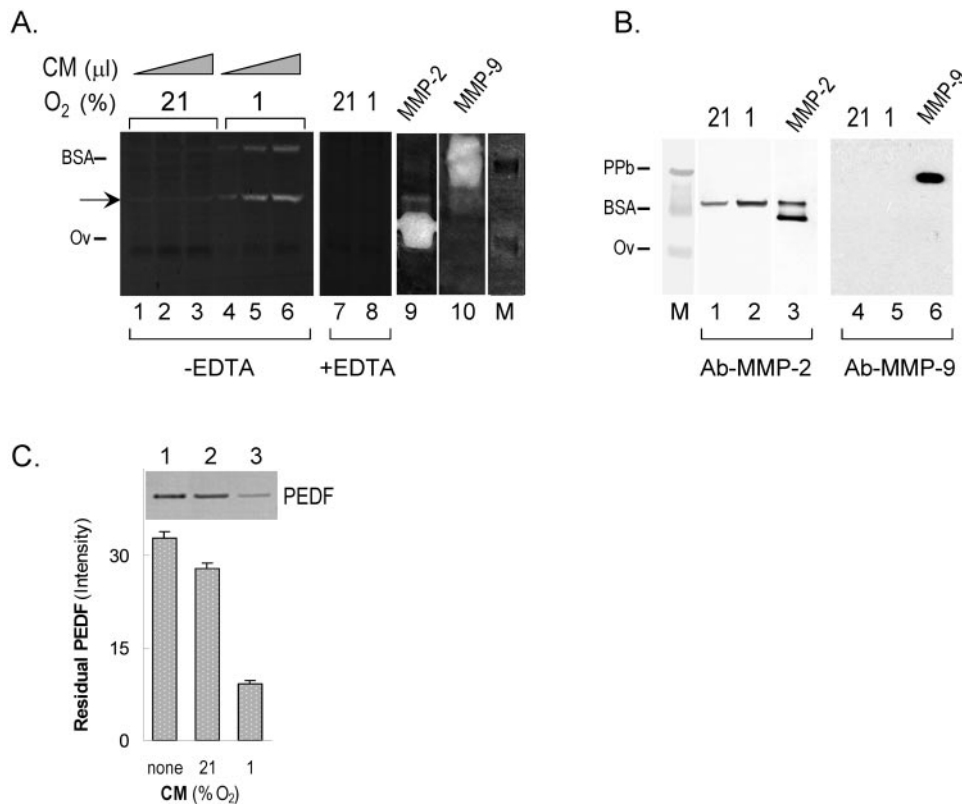


Briefly, 10-mm-long, surgical-grade silicone tubes with only one end open (angioreactors) were filled with 20  $\mu$ L of synthetic matrix alone or mixed with VEGF and/or rhuPEDF exposed to different concentrations of MMP-2 and CaCl<sub>2</sub>, as described earlier. After the matrix solidified, the angioreactors were implanted subcutaneously into the dorsal flanks of anesthetized athymic nude mice (National Cancer Institute [NCI] colony). After 11 days, the mice were injected intravenously (IV) with 25 mg/mL FITC-dextran (100  $\mu$ L/mouse; Sigma-Aldrich) 20 minutes before the angioreactors were removed. Quantitation of neovascularization in the angioreactors was determined as the amount of fluorescence trapped in the implants and was measured in a spectrophotometer (HP; Perkin Elmer Life Sciences). Eight implants were used per treatment point. This protocol was approved by the internal NIH animal committee and was in compliance with the ARVO Statement for the Use of Animals in Ophthalmic and Vision Research.

## RESULTS

### Decreased PEDF Protein Production by Hypoxic RPE

In ROP, diabetic retinopathy, and animal models of retinal and choroidal neovascularization, PEDF protein levels are reported lower than in the normal retina and vitreous.<sup>18,50</sup> Similarly, PEDF levels are lower in human retinoblastoma Weri cells exposed to hypoxia than in normoxia.<sup>15</sup> Because the RPE is the main source of the secreted PEDF into the retina, we examined the effect of hypoxia on PEDF expression in the RPE, in vivo and in vitro. We used the ROP mouse model in which vessel loss is induced by exposing the animals to 75% oxygen be-



100 ng of MMP-9. Lane M: prestained MW standards. (C) Proteolytic activities against PEDF. Exogenous rhuPEDF in excess with respect to amounts present in the media was added as a potential substrate for proteases in RPE media. Purified rhuPEDF (100 ng) was mixed in 25  $\mu$ L of the culture medium (CM) from normoxia (21% O<sub>2</sub>-) and hypoxia (1% O<sub>2</sub>-) treated cells and incubated at 37°C for 1 hour. The reaction mixtures were subjected to Western blot analysis and immunostained with Ab-rPEDF by colorimetric detection. A plot of residual rhuPEDF after the incubation is shown. A blot for each reaction is shown in the inset: rhuPEDF substrate without medium (lane 1) and rhuPEDF in media from normoxic (lane 2) or hypoxic (lane 3) cells.

tween postnatal day (P)7 and P12 (P7-P12).<sup>42</sup> On removal to normoxia at P12, the retina undergoes relative ischemia, and neovascularization and neuronal cell death are induced. During the relative ischemic period (P13-P17), the levels of PEDF protein produced by the RPE-choroid were not detectable at P13 and were only marginally detected at P17 by Western blot, but then returned to normal by P21 when hypoxia-induced retinal neovascularization is known to regress (Fig. 1). Given the technical difficulties in harvesting the small mouse RPE, data were collected from pooled choroid and RPE samples. We found no significant differences in *PEDF* mRNA expression between ROP and normoxia-treated mice. *PEDF* mRNA expression increased with developmental time in the RPE-choroid, but it was extremely low or undetectable in all layers of the mouse retina (tufts, retinal ganglion cell, inner plexiform, inner nuclear, and outer nuclear), precluding the data collection from this tissue and in agreement with the lack of detection of *PEDF* transcripts in Northern blot analysis of mouse retina reported previously.<sup>51</sup>

To investigate the effect of oxygen regulation on PEDF in cultured RPE, we exposed nontransformed monkey RPE cells to low oxygen or to hypoxia mimetics. Hypoxia decreased the levels of PEDF protein in the conditioned medium to 78.5%  $\pm$  19.6% (for 7% oxygen) and 24.6%  $\pm$  1.5% (for 1% oxygen) of the normoxic cultures, as measured by relative quantitative Western blot analysis (Fig. 2A). Similar results were obtained with hypoxia mimetics (Fig. 2B). As expected, hypoxia increased *VEGF* gene expression in the same cells (Figs. 2C, 2D). However, there was no significant difference in *PEDF* mRNA levels in hypoxia-treated or untreated RPE (Figs. 2C, 2D), suggesting that hypoxic regulation of PEDF occurred at translational or posttranslational levels.

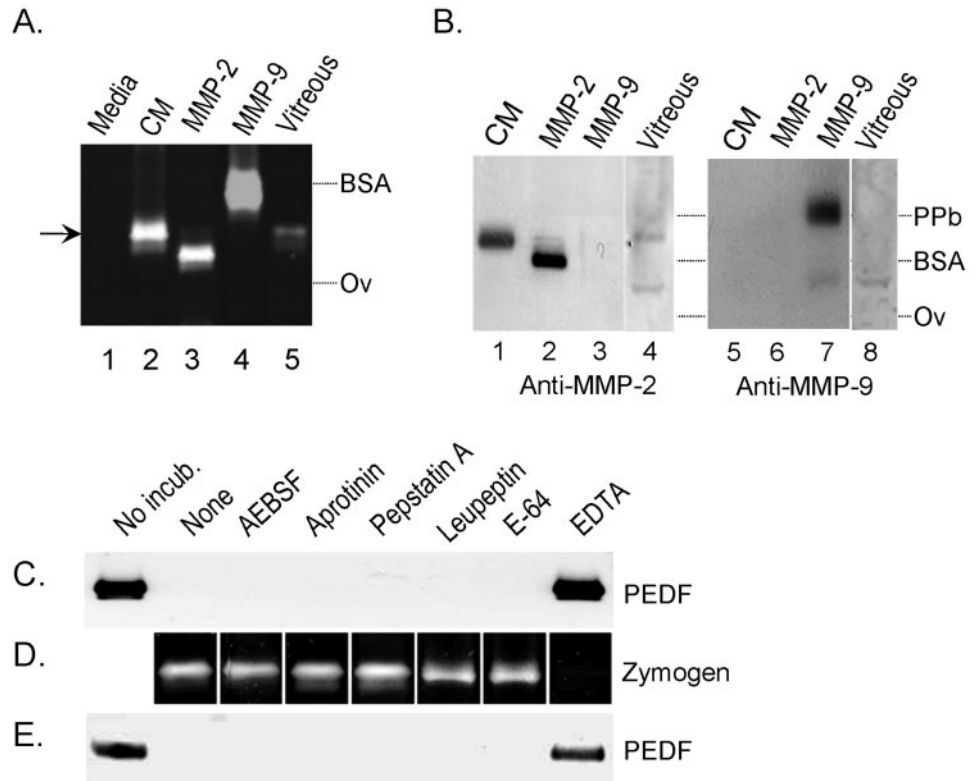
### Hypoxia-Induced PEDF-Degrading Activities in RPE

In ischemic retina, as well as in tumors, increased MMP activity controls the levels of ECM components.<sup>52,53</sup> To determine whether proteases can also regulate extracellular PEDF, we examined the effect of hypoxia on proteolytic agents secreted by RPE cells. Hypoxia increased gelatinolysis in RPE cell-conditioned media, as measured by zymography (Fig. 3A). In 10% polyacrylamide gels, these activities comigrated with MMP-2 and -9 gelatinolytic zymogens of apparent molecular weights of ~57 and ~86 kDa. We note that vitreous also exhibited ~57-kDa zymogens (Fig. 4A). The RPE gelatinolytic zymogens were activated with calcium and inhibited by EDTA, as expected for MMPs (Fig. 3A). However, only MMP-2-immunoreactive proteins were detected by Western blot analysis of the RPE media with anti-MMP-2 and anti-MMP-9 on 10% to 20% polyacrylamide gels and samples prepared under reducing conditions. The MMP-2-immunoreactive band of the RPE media comigrated with the ~72-kDa band of commercial MMP-2 (Fig. 3B). The difference of apparent molecular weights in zymography and Western blots was probably due to differences in sample preparation and SDS-PAGE conditions. The MMP-2 immunoreactive signal in the RPE media was elevated twofold by hypoxia.

To investigate the effect of RPE-derived proteolytic activities on PEDF, purified rhuPEDF was added to the RPE media at a >10-fold excess over the amounts of PEDF present in the media. After incubation for 1 hour at 37°C, the levels of exogenous rhuPEDF substrate decreased to 85% in media from normoxia-treated cells, while they were drastically lowered to 29% in media of hypoxic cells (Fig. 3C). No limiting PEDF proteolytic products were detected in the blot. Together, these

**FIGURE 3.** Hypoxia increased MMP-2 zymogens in media conditioned by RPE cells. RPE cells were exposed to various concentrations of oxygen and the culture medium (CM) from hypoxia (1% O<sub>2</sub>-) and normoxia (21% O<sub>2</sub>-) treated cells was collected. (A) Zymography. Media were concentrated 80-fold and subjected to gelatin zymography. Coomassie blue-stained gels are shown with lanes 1 to 3 and 7 corresponding to 1, 5, 10, and 10  $\mu$ L of medium from normoxic cells, respectively; lanes 4 to 6 and 8 corresponding to 1, 5, 10, and 10  $\mu$ L medium from hypoxic cells, respectively. Lanes 7 and 8 correspond to zymography in the presence of the metalloproteinase inhibitor, EDTA (60 mM). Lanes 9 and 10 correspond to commercial MMP-2 and -9. Lane M: prestained MW standards. (B) Western blot analysis. Concentrated media was subjected to Western blot analysis and immunostained with antiserum against MMP-2 by colorimetric detection (lanes 1-3) and with antiserum against MMP-9 by chemiluminescent detection (lanes 4-6). Western blot analyses are shown, with lanes 1 and 4 corresponding to medium from normoxic cells (20  $\mu$ L); lanes 2 and 5, medium from hypoxic cells (20  $\mu$ L); lane 3, 100 ng of purified MMP-2; and lane 6,

**FIGURE 4.** MMP-2 enzymatic activities in BHK[pPEDF] and vitreous. Confluent BHK[pPEDF] cells were maintained in medium without serum for 16 hours at 37°C and the conditioned medium (CM) was collected. (A) Gelatin zymography of 5  $\mu$ L of nonconditioned medium (lane 1); 5  $\mu$ L of conditioned medium (lane 2), 2 ng recombinant human MMP-2 (lane 3); 2 ng purified recombinant human MMP-9 (lane 4); and 5  $\mu$ L of homogenized monkey vitreous (lane 5). (B) Western blots of 20  $\mu$ L CM concentrated 50-fold (lanes 1 and 5); 50 ng of recombinant human MMP-2 (lanes 2 and 6); 50 ng of recombinant human MMP-9 (lanes 3 and 7), human vitreous (lanes 4 and 8), with antibodies to MMP-2 and -9, as indicated. (C, D) PEDF-degrading activity and zymography of CM, respectively, in the presence of specific proteinase inhibitors. (C) A total of 100 ng rhuPEDF (>35-fold excess over endogenous PEDF) was mixed in 10  $\mu$ L BHK CM with protease inhibitors, as indicated, and incubated at 37°C for 1 hour. Reaction mixtures were subjected to Western blot analysis and immunostained with anti-PEDF monoclonal antibodies by colorimetric detection of the residual rhuPEDF. (D) Aliquots of CM (5  $\mu$ L)



were subjected to gelatin zymography. Lanes were excised and incubated in zymography developing buffer containing each protease inhibitor indicated in (C). (E) Endogenous PEDF degradation in vitreous. Monkey vitreal fraction p70 was mixed with protease inhibitors plus 10 mM CaCl<sub>2</sub> and incubated at 37°C for 2 hours. The reaction mixtures were subjected to Western blot analysis and immunostained with Ab-rPEDF to detect residual endogenous vitreal PEDF. Western blot analysis of the vitreous clearly showed the presence of EDTA-sensitive PEDF-degrading activities similar to BHK cells. No incub., control cultures without incubation. The concentrations of protease inhibitors in each reaction were for serine proteases, 100 mM AEBSEF, and 5  $\mu$ g/mL aprotinin; for aspartic proteases, 5  $\mu$ g/mL pepstatin A; for cysteine proteases, 1 mM leupeptin; for calpain, 20  $\mu$ g/mL E-64; and for metalloproteinases, 20 mM EDTA.

results indicate that hypoxia induced MMP and gelatinase-type activities in RPE and that PEDF was sensitive to the proteolytic degradation induced by hypoxia.

### VEGF-Induced PEDF-Degrading Activities

To study the effects of MMP induction on PEDF we chose BHK[pPEDF] cells, because they express human PEDF under the control of a heterologous cytomegalovirus (CMV) promoter and secrete the recombinant PEDF protein into the culture medium. The fact that the PEDF gene is under the control of a promoter considered constitutive (e.g., lacking in transcriptional regulation of the heterologous PEDF gene) provides an advantage over primary cultures that allows mechanisms of posttranscriptional and posttranslational regulation to be revealed. Zymography and Western blot analysis of the BHK[pPEDF]-conditioned media clearly showed that these cells also secrete ~57-kDa gelatinolytic agents and ~72-kDa MMP-2 immunoreactivity, similar to those in the vitreous (Figs. 4A, 4B), and these were the only zymogens and immunoreactive bands detected. No detectable MMP-9 immunoreactivity was detected in the media. To examine the ability of proteinases secreted by BHK[pPEDF] cells to degrade PEDF, exogenous PEDF substrate was added to the media and incubated at 37°C for 1 hour. The proteolysis was characterized with specific inhibitors of metallo-, serine-, aspartic- and cysteine-proteinases. The media catalyzed the degradation of PEDF protein, which was inhibited only with the metalloproteinase inhibitor EDTA, whereas AEBSEF, aprotinin, pepstatin A, leupeptin, or E64 had no effect (Fig. 4C). This PEDF-degrading activity was

identical with that in vitreous from monkey eyes (Fig. 4E). Zymography in the presence of inhibitors also showed that only EDTA inhibited the in-gel activity of the media, correlating with the activity that degraded PEDF (Fig. 4D). These results demonstrate that BHK cells secreted PEDF-degrading members of the MMP family, similar to those in the vitreous.

The proangiogenic factor VEGF can induce the expression of MMP genes and activate MMP gelatinolytic activities.<sup>35,36</sup> In addition, VEGF is an important oxygen-regulated factor. To study the effects of VEGF on PEDF degradation, we exploited the BHK[pPEDF] cell system by adding increasing concentrations of recombinant human VEGF to the cell cultures. Incubation time (data not shown) and VEGF dose induced increases in the secreted ~57-kDa MMP-2-like zymogens, as revealed by gelatin zymography of the BHK[pPEDF] media (Fig. 5A). Conversely, the steady state levels of PEDF protein in the same media declined with VEGF dose (Fig. 5B). Note that addition of 0 to 100 nM VEGF did not affect the number of cells in the cultures (Notari L, personal observations, 2003). In addition, the VEGF dose increased the overall gelatinolysis in the media, as determined by DQ-gelatin degradation solution assays (Fig. 5C). To investigate the effects of VEGF on PEDF degradation, exogenous rhuPEDF substrate was added to the BHK[pPEDF] media at an excess of >100-fold over the endogenous PEDF. After incubation for 2 hour at 37°C, the residual rhuPEDF decreased to almost undetectable levels with VEGF treatments in a concentration-dependent fashion (Fig. 5D). Both DQ-gelatinolytic and PEDF-degrading activities of the media were sensitive to inhibition by EDTA (data not shown). These results

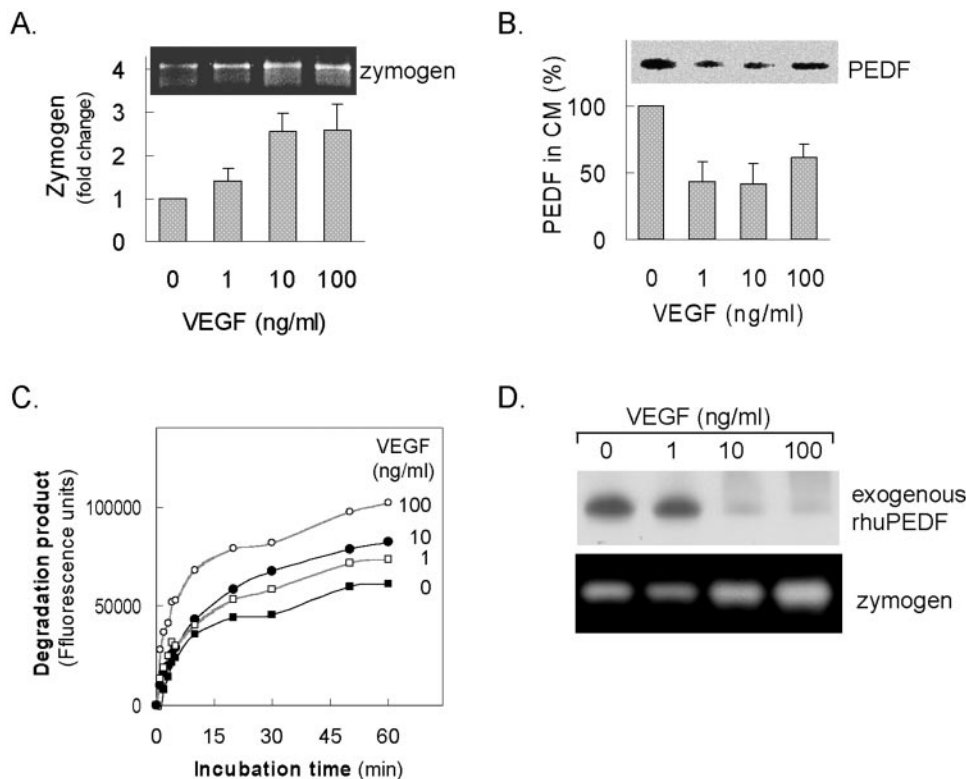


**FIGURE 5.** Effects of VEGF on gelatinolytic activities and PEDF levels in BHK[pPEDF]. BHK[pPEDF] cells were cultured in media without serum with increasing concentrations of VEGF at 37°C. Conditioned media were harvested at the indicated times and used as an enzyme source. (A, B) Levels of ~57-kDa zymogens and PEDF protein in the media from cells cultured for 8 hours with increasing VEGF concentrations, respectively. Proteases in the media (5  $\mu$ L) were resolved by gelatin zymography (*inset*), and the band intensities of the reverse zymogram gel stained with Coomassie blue were quantified and plotted versus VEGF concentrations for each treatment (A). PEDF protein levels were calculated by relative quantitative immunoblot analysis. A total of 15  $\mu$ L of each concentrated medium (50-fold) was subjected to Western blot analysis with anti-PEDF antibodies (*inset*), the band intensities for PEDF protein were determined, and the percentage of PEDF in the VEGF-treated media relative to the nontreated was plotted versus VEGF concentrations (B). (C) Solution degradation assays with DQ-gelatin substrate and media from cells treated for 24 hours with increasing VEGF concentrations. Formation of

products was followed by an increase in fluorescence derived from unquenching the DQ-gelatin substrate on proteolytic cleavages. (D) VEGF's effects on PEDF-degrading agents secreted by BHK[pPEDF] cells. Media conditioned by BHK[pPEDF] cells from 24 hours' incubation (same as in C) were collected and contained <0.5  $\mu$ g/mL PEDF. A total of 133 mg/mL exogenous rhuPEDF (an excess by >100-fold over the endogenous PEDF) and 10 mM  $\text{CaCl}_2$  were added to the media. The reaction mixtures were incubated at 37°C for 2 hours and resolved by SDS-PAGE, and the gels were stained with Coomassie blue to detect the residual PEDF (*top*). A total of 10  $\mu$ L of conditioned media were subjected to gelatin zymography (*bottom*).

demonstrate that PEDF was sensitive to the proteolytic degradation induced by VEGF and imply that MMP-like proteinases induced by VEGF mostly contributed to the degradation of PEDF. Thus, PEDF can be downregulated by VEGF-mediated induction of MMP-like activity.

### PEDF Protein as a Substrate of MMP-2 and -9

The compact and globular PEDF protein (50-kDa) is highly resistant to proteolytic cleavage except for a protease-sensitive exposed peptide loop located toward its C end.<sup>22</sup> On cleavage by serine proteases, subtilisin, or endoproteinases, the limited PEDF polypeptide products (~46 kDa) retain biological activity and binding affinity for ECM collagens and glycosaminoglycans.<sup>8,9,22</sup> To characterize the effects of MMPs on PEDF, purified rhuPEDF was treated with MMP-2 or -9 in a controlled fashion, and the reaction products analyzed by SDS-PAGE on 10% to 20% gradient polyacrylamide gels with Coomassie blue staining to favor detection of low-molecular-weight polypeptide breakdown products (Fig. 6). At a low proteinase-substrate ratio (wt/wt; 1:1000) both MMPs proteolyzed PEDF as early as 45 minutes, leaving no apparent limiting peptide products to be detected in the gel (Figs. 6A, 6D). Increasing the proteinase-PEDF ratio had an even more dramatic effect on PEDF degradation (Figs. 6B, 6E). In addition, the degrading effect of MMP-2 and -9 on PEDF was dependent on increasing concentrations of  $\text{CaCl}_2$  and sensitive to EDTA (Figs. 6C, 6F). These results clearly demonstrate that the PEDF molecule was a substrate for MMP-2 and -9 proteolytic activities and apparently was a target for proteolytic degradation rather than for proteolytic processing.

### Effect of MMP-Mediated Proteolysis on the Biological Activities of PEDF

PEDF has a role in preventing both retinal cell death and neovascularization. To examine the neuronal survival activities of PEDF proteolyzed with MMP-2, we followed a method in which neuronal cell death is induced in rat retinal neuronal R28 cells by serum deprivation.<sup>47</sup> PEDF was treated with MMP-2, as described earlier (Fig. 6C). Treatments of serum-deprived R28 cells with 100 nM PEDF (intact nonproteolyzed; Fig. 7B) versus untreated cultures (Fig. 7A) increased cell viability 2.5-fold (Fig. 7F). This survival effect decreased gradually with increased MMP-2-mediated proteolysis of PEDF as there was a dose-dependent loss of this effect with PEDF pretreated with MMP-2 and increasing  $\text{Ca}^{2+}$  concentrations (Figs. 7B-F), so that at maximum proteolysis, when no residual PEDF was detected by SDS-PAGE (Fig. 6C), cell viability matched that of control cultures not exposed to PEDF (compare Figs. 7A and 7E, and see Fig. 7F).

Similarly, the ability of PEDF to prevent neovascularization diminished with its degradation by MMP-2 (Fig. 8). The biological effects of PEDF proteolysis by MMP-2 in angiogenesis were assessed by two different methods, an ex vivo angiogenesis assay using chicken embryo aortic arch rings and an in vivo assay (DIVAA). In the chicken embryo assay, the area of sprouting new vessels greatly increased in the presence of ECGS (Fig. 8B) when compared to the untreated rings (Fig. 8A). Addition of 1 ng/ $\mu$ L intact nonproteolyzed PEDF decreased ECGS-induced angiogenesis to almost basal levels (Fig. 8C). As PEDF was proteolyzed by MMP-2 in the presence of increasing con-

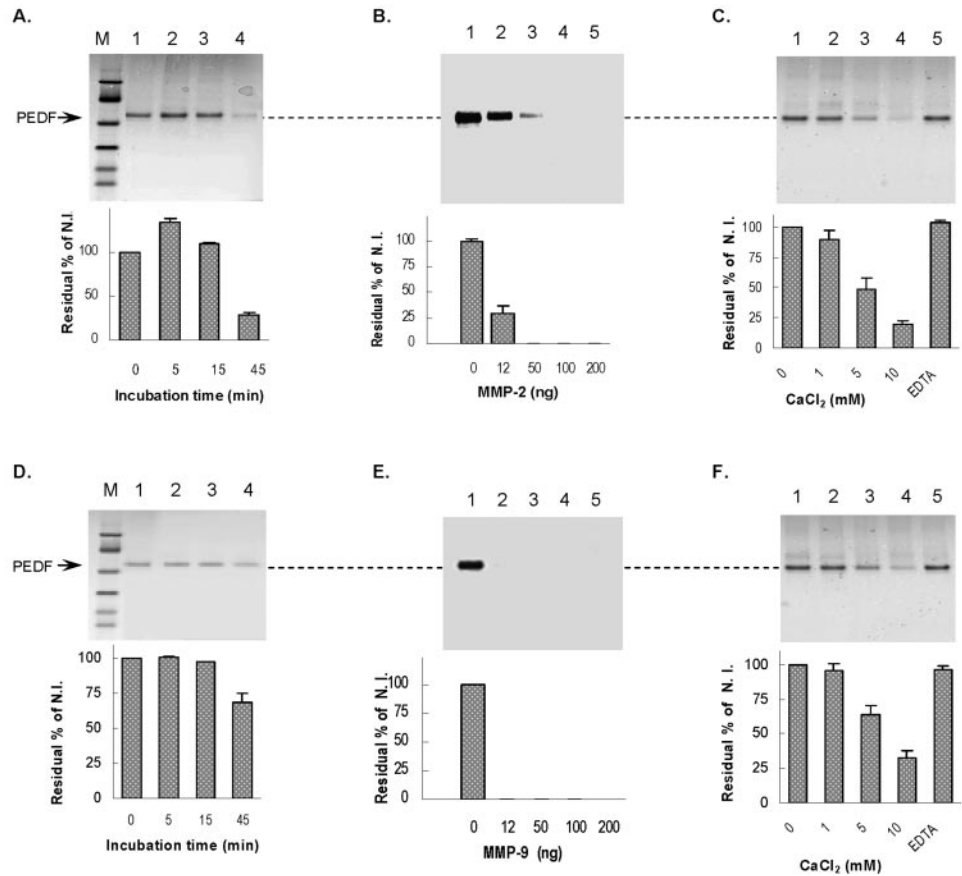


**FIGURE 6.** PEDF is a substrate for MMP-2 and -9 enzymes. Effects of incubating rhuPEDF with MMP-2 (A–C) or MMP-9 (D–F) in PBS at 37°C. (A, D) Time-course treatments. Reactions were with rhuPEDF (2  $\mu$ g) and 2 ng of enzyme in the presence of 7.5 mM CaCl<sub>2</sub>, and incubations were for the indicated periods (lanes 1–4). (B, E) Effect of increasing the protease-substrate ratio. Reactions were with 100 ng rhuPEDF, 5 mM CaCl<sub>2</sub>, and the indicated amounts of protease, and incubation was for 1 hour. (C, F) Effect of CaCl<sub>2</sub>. Reactions with 2  $\mu$ g rhuPEDF and 2 ng enzyme were incubated for 1 hour in the presence of CaCl<sub>2</sub> concentrations, as indicated (lanes 1–4), or in the presence of 20 mM EDTA and 10 mM CaCl<sub>2</sub> (lane 5). Residual rhuPEDF in reactions mixtures after treatment was resolved by SDS-PAGE and detected either by Coomassie blue staining (A, B, D, E) or immunostaining in Western blots with anti-PEDF monoclonal antibodies and colorimetric detection (C, F). Lane M: prestained SDS-PAGE standards, low range.

centrations of Ca<sup>2+</sup>, the antiangiogenic effect of PEDF was progressively lowered (Figs. 8D–G). Similar results were observed in the DIVAA test (Fig. 8H) with 10 nM VEGF as an angiogenic promoter. Again, intact nonproteolyzed PEDF had a dramatic effect in diminishing VEGF-induced angiogenesis, and there was a dose-dependent loss of this effect with PEDF pretreated with MMP-2 and increasing Ca<sup>2+</sup> concentrations. These results showed that the PEDF products of MMP-2 digestion did not contain structural determinants for PEDF biological activities; thus, MMP-2-mediated proteolysis abolished PEDF's retinal survival and antiangiogenic properties.

## DISCUSSION

In the current study, hypoxia caused a decline of PEDF by extracellular MMP-mediated proteolytic degradation, and we propose that hypoxia induction of gelatinaseA/MMP-2 and/or gelatinase B/MMP-9 diminishes levels of PEDF protein and lead to an increase in the potential for angiogenesis and/or neuronal cell death in the retina. Several lines of evidence support this conclusion. First, hypoxia had a marked effect on decreasing the levels of PEDF produced by RPE cells, without affecting the *PEDF* mRNA levels, similar to that observed with retinoblastoma Weri cells.<sup>15</sup> Second, our results demonstrate that PEDF was sensitive to proteolytic degradation induced by hypoxia or VEGF. Third, the PEDF-degrading activities induced by both hypoxia and VEGF exhibited characteristics of the MMP class of proteinases. Fourth, MMP-2 and -9 catalyzed the Ca<sup>2+</sup>-dependent proteolytic degradation of PEDF. Fifth, MMP-2-mediated degradation of PEDF resulted in biologically inactive products in retinal survival and angiogenesis assays.

The fact that PEDF is a substrate target for MMP-2 and -9 is consistent with mechanisms for regulation of PEDF at a post-

translational level and occurring outside of the cell in the ECM. The observed decline of PEDF by hypoxia is most likely an effect of increased proteolytic activities by MMP inducers (e.g., VEGF). It has been shown that MMP-2 and -9 act on VEGF by releasing the protein from ECM storage rather than degrading it and increasing its availability.<sup>26</sup> We envision a novel mechanism for PEDF downregulation by hypoxia that involves PEDF proteolysis mediated by MMPs, which target PEDF among several other ECM protein components, resulting in loss of its biological activities. This mechanism explains hypoxia-provoked increases in VEGF-PEDF ratios and suggests that MMP-mediated PEDF degradation might form part of the angiogenic switch and prevent neuronal survival in the retina.

Our results have biochemical implications. The effects of hypoxia on VEGF expression as well as the effects of VEGF on MMP-2 and -9 gene expression and on MMP-2 and -9 proteolytic activity have been shown by others.<sup>35,36</sup> However, a single recognition cleavage site for these proteinases is not known. Most conventional substrates for MMP-2 or -9 are degraded rather than processed and more than 15 cleavage recognition sites are known in numerous substrates. The common feature is the presence of a hydrophobic amino acid residue at the amino end of the cleavage site (e.g., valine, leucine, isoleucine, or phenylalanine). The amino acid sequence of the mature human PEDF has more than 100 hydrophobic residues, including 24 valines, 51 leucines, 21 isoleucines, 18 phenylalanines, and 10 tyrosines residues and shares several MMP-2 or -9 cleavage sites identified in other substrates. Most of the proteinases cleave the highly ordered globular PEDF protein at its homologous serpin-reactive loop, leaving an active core polypeptide molecule as a limited product.<sup>22</sup> However, MMP-2 and -9 degrade PEDF to peptides, contrasting with many other inhibitory serpins in which inactivation is achieved by cleavage



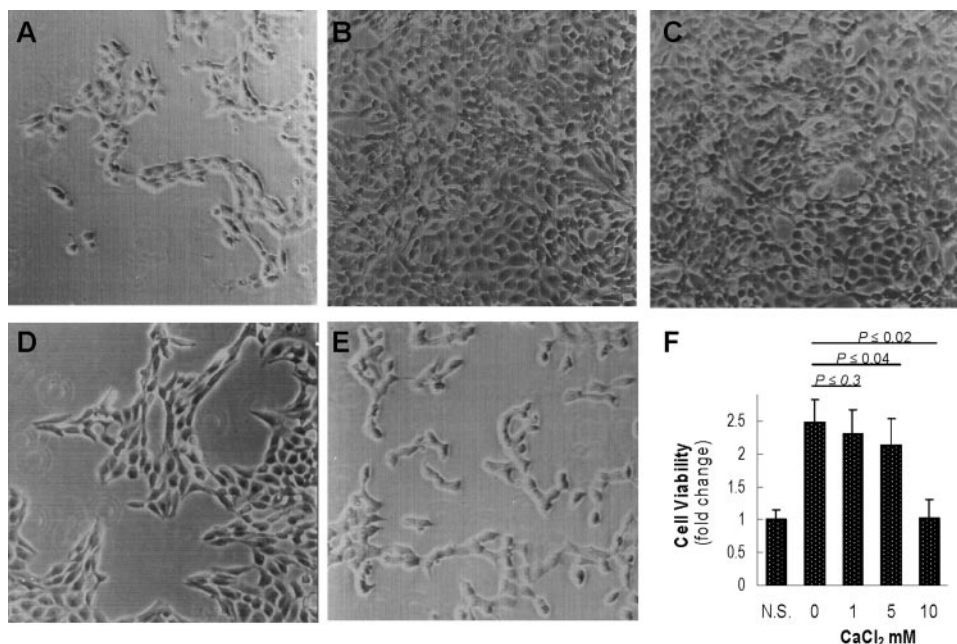


**FIGURE 7.** Retinal cell survival assays of MMP-2-treated PEDF. Retinal neuronal R28 cells were cultured in 24-well plates to 70% confluence and deprived of serum for 72 hours to induce cell death by apoptosis. (A) Reaction mixtures of rhuPEDF and MMP-2 were incubated at a substrate-protease ratio of 1000:1 in the presence of increasing concentrations of CaCl<sub>2</sub> (as described in Fig. 6C) and then added to the cultures at a PEDF substrate concentration of 100 nM. (A-E) Representative fields of R28 cells treated with rhuPEDF-MMP-2 reaction mixtures without CaCl<sub>2</sub> (B), 1 mM CaCl<sub>2</sub> (C), 5 mM CaCl<sub>2</sub> (D), 10 mM CaCl<sub>2</sub> (E), and serum-deprived control without PEDF (A). (F) Quantification of R28 cell viability with MMP-2-treated rhuPEDF at increasing CaCl<sub>2</sub> concentrations. Data are the mean ± SD of results in four independent experiments with different batches of R28 cells, each with more than three replicates per assay. No significant difference was observed between values for NS vs. 10 mM CaCl<sub>2</sub> as determined by *t*-test. NS, no serum, control without PEDF.

at the serpin-reactive loop.<sup>54,55</sup> Besides the serpin-exposed loop, the crystal structure of PEDF reveals more than 10 cleavage sites partially exposed in the folded polypeptide and available for an attack by MMP-2 (Notari L, Becerra SP, personal observations, 2004). We propose that on substrate binding, MMP-2 and/or -9 induced an unfolding of the PEDF protein that increases the availability of several sites to leave products that lack neurotrophic or antiangiogenic properties. Thus, it seems that MMP inactivation of serpins is achieved by different mech-

anisms. Although MMPs can inactivate inhibitory serpins (e.g., antitrypsin and antithrombin III) by attacking the serpin-reactive loop, the loss of PEDF biological activities is achieved by complete proteolysis.

Our results offer further insight into the stimulation of angiogenesis by a high dose of PEDF in a CNV model, as described by Apte et al.<sup>56</sup> They showed that increasing the concentrations of exogenous PEDF can stimulate VEGF production by endothelial cells in a linear and dose-dependent

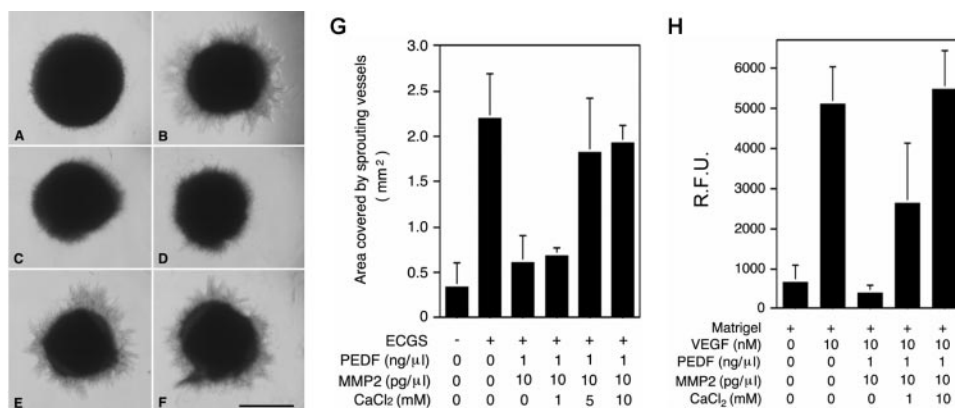


**FIGURE 8.** Antiangiogenic activity of MMP-2-treated PEDF. Photographs of chicken embryo aortic arch rings embedded in synthetic matrix and exposed to different angiogenic solutions for 24 hours (A-F). The negative control (A) shows insignificant sprouting, whereas the positive control containing 400 μg/mL ECGS (B) displays a full crown of new vessels. The other rings were treated with 1 ng/μL rhuPEDF that had been incubated in the presence of 10 pg/μL MMP-2 and 0 (C), 1 (D), 5 (E), or 10 (F) mM CaCl<sub>2</sub>. Bar, 1 mm. (G) Quantification of the area covered by the sprouting vessels in the chicken embryo aortic arch ring angiogenesis

assay. The treatments were as described in the previous panels. Data are the mean ± SD of six independent measurements. (H) Quantification of the DIVAA performed in mice. Angioreactors containing 20 μL of synthetic matrix plus bioactive substances, as indicated, were placed under the skin of nude mice for 11 days. After intravenous injection of FITC-dextran, the amount of fluorescence trapped within the angioreactor provided a measurement of the volume of blood circulating through the newly formed vessels. Data are the mean ± SD of eight independent measurements. R.F.U., relative fluorescence units.

manner. The stimulated VEGF can induce MMP-2 and -9, as has been shown for several types of cells by other investigators and in the present study.<sup>34–36</sup> On secretion and activation, these MMPs can degrade ECM components including PEDF (Figs. 5, 6), but not VEGF.<sup>26</sup> The overall response of a high dose of PEDF would be MMP-mediated proteolytic inactivation of PEDF that leads to an increase in the VEGF-PEDF ratio and stimulation of angiogenesis. However, a high dose of PEDF would not necessarily result in a decrease of neurotrophic activity. There is increasing evidence of neurotrophic activity of VEGF<sup>57–59</sup> and thus the stimulated VEGF could complement PEDF's neurotrophic activities in the retina. It is worth mentioning that the concentrations of PEDF that stimulated VEGF production in endothelial cells<sup>56</sup> were significantly higher than those in physiological vitreous from several species.<sup>4,18,38,44,60,61</sup> We also asked whether intravitreal injections of PEDF would inhibit retinal neovascularization in the ROP model (Smith LEH, Robinson G, personal observations, 2002). However, in contrast to data reported by Stellmach et al.<sup>12</sup> with 22.4  $\mu$ g PEDF administered intraperitoneally, we did not observe inhibition of retinal neovascularization with intravitreal injections of 1  $\mu$ g PEDF, which were the identical route and amounts used successfully for protection of photoreceptors in *rd* and *rds* mice<sup>62</sup> and double the amount used in rats with light-induced damage.<sup>10</sup> The regulation of VEGF by oxygen in a model of ROP has been reported previously by one of our laboratories and many others.<sup>63–65</sup> The expression of VEGF in retinas from an ROP mouse model after transfer to normoxic conditions is upregulated and correlates with development of neovascularization. There is increasing evidence of the modulation of MMP-2 and -9 in the ROP model (see reviews by Sivak and Fini<sup>53</sup> and by Das and McGuire<sup>23</sup>). In summary, levels of MMP-2 and -9 zymogens and mRNA in retina significantly increase with induced retinal neovascularization in the ROP model (mouse and rat) and neovascularization can be significantly inhibited with intraperitoneal administration of an MMP-2 and -9 inhibitor.<sup>66–68</sup> The angiogenic effect observed with a high dose of PEDF may be due to stimulation of MMP-mediated PEDF degradation in addition to VEGF stimulation. Thus, it is envisioned that including MMP inhibitors along with high doses of PEDF may prevent the MMP-mediated degradation triggered by this cascade and stimulation of angiogenesis.

Our results also have clinical implications. Tissue hypoxia and/or neural loss occurs in retinal diseases, such as diabetic retinopathy, ROP, retinal detachment, age-related macular degeneration, glaucoma, and tumor growth, and adversely affects quality of life.<sup>69–71</sup> Although oxygen deprivation is an early stimulus for neovascularization and cell injury, the molecular signals for the pathologic development of new vessels and neuronal cell death are not fully defined. Induction of angiogenic factors and extracellular matrix degradation stimulate angiogenesis and cell injury.<sup>72,73</sup> Whereas VEGF and MMP-2 and -9 are important in choroidal and retinal neovascularization, and in RGC death,<sup>27,53,74</sup> prevention of angiogenesis and retinal cell death are associated with increases of antiangiogenic and neurotrophic factors—one being PEDF, the principal antiangiogenic and neurotrophic protein of the eye.<sup>1–3</sup> Evidence that supports a role of MMPs in modulating the activities of PEDF in the eye is increasing.<sup>53</sup> In diabetic retinopathy and ROP animal models, the ischemic retina has upregulated MMP-2 and -9 and lower levels of PEDF compared with physiological conditions.<sup>15,18,53</sup> MMP-2 and PEDF are present in the interphotoreceptor matrix, and while the interphotoreceptor matrix MMP-2 (gelatinase A) increases with age-related macular degeneration, there is a decrease in retinal PEDF levels associated with this disease.<sup>25,75</sup> Inhibitors of MMPs decrease retinal neovascularization in ROP mouse models<sup>66</sup> and are being clinically tested as novel therapies for

age-related macular degeneration, predicting an increase in PEDF.<sup>76</sup> The fact that in MMP-9-null mice the RGCs do not die when injured by ischemia<sup>28</sup> would point to an increase in PEDF levels in the RGC layer due to lack of PEDF degradation by the ablated MMP-9. A decrease in retinal angiogenesis is identified in MMP-2-null mice,<sup>77</sup> consistent with the involvement of MMP-2 in degrading PEDF in retinal neovascularization. In double MMP-2- and -9-null mice,<sup>27</sup> and in wild-type mice treated with gelatinase specific inhibitors, choroidal neovascularization is inhibited, again consistent with decreased degradation of the antiangiogenic PEDF. Evidence also exists for photoreceptor cell death induced by hypoxia at early developmental stages<sup>78</sup> and suggests that MMPs induced by hypoxia degrade PEDF, a survival factor for photoreceptors. Thus, inhibition of PEDF degradation would be beneficial for the treatment of different forms of vascular and neuronal ocular diseases, and direct administration of PEDF could be more effective if accompanied by MMP inhibitors.

### Acknowledgments

The authors thank Liz Perruccio for discussions of gelatin-affinity column chromatography and Christina Meyer and Natalia Balko for technical assistance with proteolysis assays.

### References

1. Bouck N. PEDF: anti-angiogenic guardian of ocular function. *Trends Mol Med.* 2002;8:330–334.
2. Tombran-Tink J, Barnstable CJ. PEDF: a multifaceted neurotrophic factor. *Nat Rev Neurosci.* 2003;4:628–636.
3. King GL, Suzuma K. Pigment-epithelium-derived factor: a key co-ordinator of retinal neuronal and vascular functions. *N Engl J Med.* 2000;342:349–351.
4. Becerra SP, Fariss RN, Wu YQ, et al. Pigment epithelium-derived factor in the monkey retinal pigment epithelium and interphotoreceptor matrix: apical secretion and distribution. *Exp Eye Res.* 2004;78:223–234.
5. Perez-Mediavilla LA, Chew C, Campochiaro PA, et al. Sequence and expression analysis of bovine pigment epithelium-derived factor. *Biochim Biophys Acta.* 1998;1398:203–214.
6. Tombran-Tink J, Shivaram SM, Chader GJ, et al. Expression, secretion, and age-related downregulation of pigment epithelium-derived factor, a serpin with neurotrophic activity. *J Neurosci.* 1995;15:4992–5003.
7. Yasui N, Mori T, Morito D, et al. Dual-site recognition of different extracellular matrix components by anti-angiogenic/neurotrophic serpin, PEDF. *Biochemistry.* 2003;42:3160–3167.
8. Meyer C, Notari L, Becerra SP. Mapping the type I collagen-binding site on pigment epithelium-derived factor. Implications for its antiangiogenic activity. *J Biol Chem.* 2002;277:45400–45407.
9. Alberdi E, Hyde CC, Becerra SP. Pigment epithelium-derived factor (PEDF) binds to glycosaminoglycans: analysis of the binding site. *Biochemistry.* 1998;37:10643–10652.
10. Cao W, Tombran-Tink J, Chen W, et al. Pigment epithelium-derived factor protects cultured retinal neurons against hydrogen peroxide-induced cell death. *J Neurosci Res.* 1999;57:789–800.
11. Mori K, Duh E, Gehlbach P, et al. Pigment epithelium-derived factor inhibits retinal and choroidal neovascularization. *J Cell Physiol.* 2001;188:253–263.
12. Stellmach V, Crawford SE, Zhou W, et al. Prevention of ischemia-induced retinopathy by the natural ocular antiangiogenic agent pigment epithelium-derived factor. *Proc Natl Acad Sci USA.* 2001;98:2593–2597.
13. Takita H, Yoneya S, Gehlbach PL, et al. Retinal neuroprotection against ischemic injury mediated by intraocular gene transfer of pigment epithelium-derived factor. *Invest Ophthalmol Vis Sci.* 2003;44:4497–4504.
14. Wang L, Schmitz V, Perez-Mediavilla A, et al. Suppression of angiogenesis and tumor growth by adenoviral-mediated gene transfer of pigment epithelium-derived factor. *Mol Ther.* 2003;8:72–79.

15. Dawson DW, Volpert OV, Gillis P, et al. Pigment epithelium-derived factor: a potent inhibitor of angiogenesis. *Science*. 1999; 285:245-248.
16. Gao G, Li Y, Fant J, et al. Difference in ischemic regulation of vascular endothelial growth factor and pigment epithelium-derived factor in brown Norway and Sprague Dawley rats contributing to different susceptibilities to retinal neovascularization. *Diabetes*. 2002;51:1218-1225.
17. Renno RZ, Youssri AI, Michaud N, et al. Expression of pigment epithelium-derived factor in experimental choroidal neovascularization. *Invest Ophthalmol Vis Sci*. 2002;43:1574-1580.
18. Spranger J, Osterhoff M, Reimann M, et al. Loss of the antiangiogenic pigment epithelium-derived factor in patients with angiogenic eye disease. *Diabetes*. 2001;50:2641-2645.
19. Becerra SP. Structure-function studies on PEDF: a noninhibitory serpin with neurotrophic activity. *Adv Exp Med Biol*. 1997;425: 223-237.
20. Gettins PG, Simonovic M, Volz K. Pigment epithelium-derived factor (PEDF), a serpin with potent anti-angiogenic and neurite outgrowth-promoting properties. *Biol Chem*. 2002;383:1677-1682.
21. Simonovic M, Gettins PG, Volz K. Crystal structure of human PEDF, a potent anti-angiogenic and neurite growth-promoting factor. *Proc Natl Acad Sci USA*. 2001;98:11131-11135.
22. Becerra SP, Sagasti A, Spinella P, et al. Pigment epithelium-derived factor behaves like a noninhibitory serpin: neurotrophic activity does not require the serpin reactive loop. *J Biol Chem*. 1995;270: 25992-25999.
23. Das A, McGuire PG. Retinal and choroidal angiogenesis: pathophysiology and strategies for inhibition. *Prog Retin Eye Res*. 2003; 22:721-748.
24. Noda K, Ishida S, Inoue M, et al. Production and activation of matrix metalloproteinase-2 in proliferative diabetic retinopathy. *Invest Ophthalmol Vis Sci*. 2003;44:2163-2170.
25. Plantner JJ, Jiang C, Smine A. Increase in interphotoreceptor matrix gelatinase A (MMP-2) associated with age-related macular degeneration. *Exp Eye Res*. 1998;67:637-645.
26. Bergers G, Brekken R, McMahon G, et al. Matrix metalloproteinase-9 triggers the angiogenic switch during carcinogenesis. *Nat Cell Biol*. 2000;2:737-744.
27. Lambert V, Wielockx B, Munaut C, et al. MMP-2 and MMP-9 synergize in promoting choroidal neovascularization. *FASEB J*. 2003;17:2290-2292.
28. Chintala SK, Zhang X, Austin JS, et al. Deficiency in matrix metalloproteinase gelatinase B (MMP-9) protects against retinal ganglion cell death after optic nerve ligation. *J Biol Chem*. 2002;277:47461-47468.
29. Brinckerhoff CE, Matrisian LM. Matrix metalloproteinases: a tail of a frog that became a prince. *Nat Rev Mol Cell Biol*. 2002;3:207-214.
30. Sternlicht MD, Werb Z. How matrix metalloproteinases regulate cell behavior. *Annu Rev Cell Dev Biol*. 2001;17:463-516.
31. McCawley LJ, Matrisian LM. Matrix metalloproteinases: they're not just for matrix anymore! *Curr Opin Cell Biol*. 2001;13:534-540.
32. Semenza GL. HIF-1: using two hands to flip the angiogenic switch. *Cancer Metastasis Rev*. 2000;19:59-65.
33. Semenza GL. Angiogenesis in ischemic and neoplastic disorders. *Annu Rev Med*. 2003;54:17-28.
34. Wary KK, Thakker GD, Humtsoe JO, et al. Analysis of VEGF-responsive genes involved in the activation of endothelial cells. *Mol Cancer*. 2003;2:25.
35. Lamoreaux WJ, Fitzgerald ME, Reiner A, et al. Vascular endothelial growth factor increases release of gelatinase A and decreases release of tissue inhibitor of metalloproteinases by microvascular endothelial cells in vitro. *Microvasc Res*. 1998;55:29-42.
36. Burbidge MF, Coge F, Galizzi JP, et al. The role of the matrix metalloproteinases during in vitro vessel formation. *Angiogenesis*. 2002;5:215-226.
37. Ohno-Matsui K, Morita I, Tombran-Tink J, et al. Novel mechanism for age-related macular degeneration: an equilibrium shift between the angiogenesis factors VEGF and PEDF. *J Cell Physiol*. 2001;189: 323-333.
38. Ogata N, Nishikawa M, Nishimura T, et al. Unbalanced vitreous levels of pigment epithelium-derived factor and vascular endothelial growth factor in diabetic retinopathy. *Am J Ophthalmol*. 2002; 134:348-353.
39. Hanahan D, Folkman J. Patterns and emerging mechanisms of the angiogenic switch during tumorigenesis. *Cell*. 1996;86:353-364.
40. Stratikos E, Alberdi E, Gettins PG, et al. Recombinant human pigment epithelium-derived factor (PEDF): characterization of PEDF overexpressed and secreted by eukaryotic cells. *Protein Sci*. 1996;5:2575-2582.
41. Zhang JW, Gottschall PE. Zymographic measurement of gelatinase activity in brain tissue after detergent extraction and affinity-support purification. *J Neurosci Methods*. 1997;76:15-20.
42. Smith LE, Wesolowski E, McLellan A, et al. Oxygen-induced retinopathy in the mouse. *Invest Ophthalmol Vis Sci*. 1994;35:101-111.
43. Garayoa M, Martinez A, Lee S, et al. Hypoxia-inducible factor-1 (HIF-1) up-regulates adrenomedullin expression in human tumor cell lines during oxygen deprivation: a possible promotion mechanism of carcinogenesis. *Mol Endocrinol*. 2000;14:848-862.
44. Wu YQ, Becerra SP. Proteolytic activity directed toward pigment epithelium-derived factor in vitreous of bovine eyes: implications of proteolytic processing. *Invest Ophthalmol Vis Sci*. 1996;37: 1984-1993.
45. Plantner JJ, Smine A, Quinn TA. Matrix metalloproteinases and metalloproteinase inhibitors in human interphotoreceptor matrix and vitreous. *Curr Eye Res*. 1998;17:132-140.
46. Wu YQ, Notario V, Chader GJ, et al. Identification of pigment epithelium-derived factor in the interphotoreceptor matrix of bovine eyes. *Protein Expr Purif*. 1995;6:447-456.
47. Barber AJ, Nakamura M, Wolpert EB, et al. Insulin rescues retinal neurons from apoptosis by a phosphatidylinositol 3-kinase/Akt-mediated mechanism that reduces the activation of caspase-3. *J Biol Chem*. 2001;276:32814-32821.
48. Martinez A, Zudaire E, Portal-Nunez S, et al. Proadrenomedullin NH2-terminal 20 peptide is a potent angiogenic factor, and its inhibition results in reduction of tumor growth. *Cancer Res*. 2004; 64:6489-6494.
49. Martinez A, Vos M, Guedez L, et al. The effects of adrenomedullin overexpression in breast tumor cells. *J Natl Cancer Inst*. 2002;94: 1226-1237.
50. Holekamp NM, Bouck N, Volpert O. Pigment epithelium-derived factor is deficient in the vitreous of patients with choroidal neovascularization due to age-related macular degeneration. *Am J Ophthalmol*. 2002;134:220-227.
51. Singh VK, Chader GJ, Rodriguez IR. Structural and comparative analysis of the mouse gene for pigment epithelium-derived factor (PEDF). *Mol Vis*. 1998;4:7.
52. Lynch CC, Matrisian LM. Matrix metalloproteinases in tumor-host cell communication. *Differentiation*. 2002;70:561-573.
53. Sivak JM, Fini ME. MMPs in the eye: emerging roles for matrix metalloproteinases in ocular physiology. *Prog Retin Eye Res*. 2002; 21:1-14.
54. Liu Z, Zhou X, Shapiro SD, et al. The serpin alpha1-proteinase inhibitor is a critical substrate for gelatinase B/MMP-9 in vivo. *Cell*. 2000;102:647-655.
55. Mast AE, Enghild JJ, Nagase H, et al. Kinetics and physiologic relevance of the inactivation of alpha 1-proteinase inhibitor, alpha 1-antichymotrypsin, and antithrombin III by matrix metalloproteinases-1 (tissue collagenase), -2 (72-kDa gelatinase/type IV collagenase), and -3 (stromelysin). *J Biol Chem*. 1991;266:15810-15816.
56. Apte RS, Barreiro RA, Duh E, et al. Stimulation of neovascularization by the anti-angiogenic factor PEDF. *Invest Ophthalmol Vis Sci*. 2004;45:4491-4497.
57. Brockington A, Lewis C, Wharton S, et al. Vascular endothelial growth factor and the nervous system. *Neuropathol Appl Neurobiol*. 2004;30:427-446.
58. Carmeliet P, Storkebaum E. Vascular and neuronal effects of VEGF in the nervous system: implications for neurological disorders. *Semin Cell Dev Biol*. 2002;13:39-53.

59. Yourey PA, Gohari S, Su JL, et al. Vascular endothelial cell growth factors promote the in vitro development of rat photoreceptor cells. *J Neurosci*. 2000;20:6781-6788.
60. Duh EJ, Yang HS, Haller JA, et al. Vitreous levels of pigment epithelium-derived factor and vascular endothelial growth factor: implications for ocular angiogenesis. *Am J Ophthalmol*. 2004;137:668-674.
61. Ogata N, Tombran-Tink J, Nishikawa M, et al. Pigment epithelium-derived factor in the vitreous is low in diabetic retinopathy and high in rhegmatogenous retinal detachment. *Am J Ophthalmol*. 2001;132:378-382.
62. Cayouette M, Smith SB, Becerra SP, et al. Pigment epithelium-derived factor delays the death of photoreceptors in mouse models of inherited retinal degenerations. *Neurobiol Dis*. 1999;6:523-532.
63. Pierce EA, Foley ED, Smith LE. Regulation of vascular endothelial growth factor by oxygen in a model of retinopathy of prematurity. *Arch Ophthalmol*. 1996;114:1219-1228.
64. Smith LE. Pathogenesis of retinopathy of prematurity. *Growth Horm IGF Res*. 2004;14(suppl A):S140-S144.
65. Miyamoto N, Mandai M, Takagi H, et al. Contrasting effect of estrogen on VEGF induction under different oxygen status and its role in murine ROP. *Invest Ophthalmol Vis Sci*. 2002;43:2007-2014.
66. Das A, McLamore A, Song W, et al. Retinal neovascularization is suppressed with a matrix metalloproteinase inhibitor. *Arch Ophthalmol*. 1999;117:498-503.
67. Majka S, McGuire P, Colombo S, et al. The balance between proteinases and inhibitors in a murine model of proliferative retinopathy. *Invest Ophthalmol Vis Sci*. 2001;42:210-215.
68. Zhang X, Sakamoto T, Hata Y, et al. Expression of matrix metalloproteinases and their inhibitors in experimental retinal ischemia-reperfusion injury in rats. *Exp Eye Res*. 2002;74:577-584.
69. Wangsa-Wirawan ND, Linsenmeier RA. Retinal oxygen: fundamental and clinical aspects. *Arch Ophthalmol*. 2003;121:547-557.
70. Osborne NN, Melena J, Chidlow G, et al. A hypothesis to explain ganglion cell death caused by vascular insults at the optic nerve head: possible implication for the treatment of glaucoma. *Br J Ophthalmol*. 2001;85:1252-1259.
71. Kaushik S, Pandav SS, Ram J. Neuroprotection in glaucoma. *J Postgrad Med*. 2003;49:90-95.
72. Heissig B, Hattori K, Friedrich M, et al. Angiogenesis: vascular remodeling of the extracellular matrix involves metalloproteinases. *Curr Opin Hematol*. 2003;10:136-141.
73. Siao CJ, Tsirka SE. Extracellular proteases and neuronal cell death. *Cell Mol Biol (Noisy-le-grand)*. 2002;48:151-161.
74. Aiello LP, Pierce EA, Foley ED, et al. Suppression of retinal neovascularization in vivo by inhibition of vascular endothelial growth factor (VEGF) using soluble VEGF-receptor chimeric proteins. *Proc Natl Acad Sci USA*. 1995;92:10457-10461.
75. Jones BE, Moshlyedi P, Gallo S, et al. Characterization and novel activation of 72-kDa metalloproteinase in retinal interphotoreceptor matrix and Y-79 cell culture medium. *Exp Eye Res*. 1994;59:257-269.
76. Holz FG and Miller DW. Pharmacological therapy for age-related macular degeneration: current developments and perspectives [in German]. *Ophthalmologe*. 2003;100:97-103.
77. Ohno-Matsui K, Uetama T, Yoshida T, et al. Reduced retinal angiogenesis in MMP-2-deficient mice. *Invest Ophthalmol Vis Sci*. 2003;44:5370-5375.
78. Maslim J, Valter K, Egensperger R, et al. Tissue oxygen during a critical developmental period controls the death and survival of photoreceptors. *Invest Ophthalmol Vis Sci*. 1997;38:1667-1677.